



Seasonal profiles of atmospheric PAHs in an e-waste dismantling area and their associated health risk considering bioaccessible PAHs in the human lung

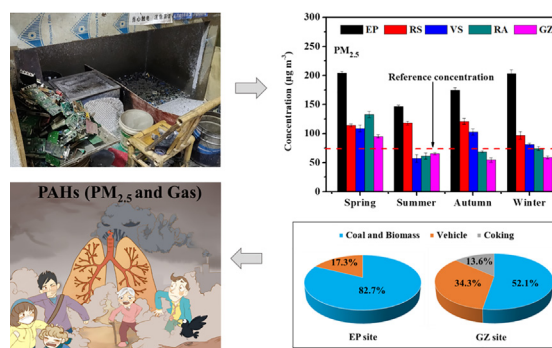
Haojia Chen, Shengtao Ma, Yingxin Yu, Ranran Liu, Guiying Li, Haibin Huang, Taicheng An *

Guangzhou Key Laboratory of Environmental Catalysis and Pollution Control, Guangdong Key Laboratory of Environmental Catalysis and Health Risk Control, School of Environmental Science and Engineering, Institute of Environmental Health and Pollution Control, Guangdong University of Technology, Guangzhou, 510006, Guangdong, China

HIGHLIGHTS

- PAH levels in spring and winter were higher than those in summer and autumn.
- The e-waste dismantling was the main source of PAHs in e-waste dismantling area.
- Low ring PAHs were significant higher in e-waste dismantling area than urban site.
- The cancer risks of atmospheric PAHs were noteworthy at EP and RA site.
- Infants suffered higher human health risk from atmospheric PAHs than adults.

GRAPHICAL ABSTRACT



ARTICLE INFO

Article history:

Received 5 March 2019
 Received in revised form 24 April 2019
 Accepted 26 April 2019
 Available online 28 April 2019

Editor: Jay Gan

Keywords:

Bioaccessibility
 E-waste dismantling
 Health risk
 Polycyclic aromatic hydrocarbon
 Seasonal variation

ABSTRACT

Due to the development of the economy, electronic waste (e-waste) has become a new global problem and e-waste dismantling processes are an important source of air pollution. Among the pollutants emitted, polycyclic aromatic hydrocarbons (PAHs) are a severe concern because of their carcinogenic and mutagenic properties. However, few studies have investigated the atmospheric PAHs generated by e-waste dismantling in a specific region, especially the PAH levels throughout the year. Thus, we assessed the effects of PAHs on the local air quality by sampling the total suspended particulates (TSP), PM₁₀, PM_{2.5}, and gaseous phase from an e-waste dismantling area and a control site during four seasons. The TSP, PM₁₀, and PM_{2.5} concentrations were measured as 84.8–414, 70.7–302, and 57.1–204 µg m⁻³, respectively, in this area, and those of three types of particulate bound-PAHs and gaseous phase PAHs were 2.6–16.1, 2.2–15.1, 1.9–14.6, and 20.1–72.8 ng m⁻³, respectively. The pollutant levels were higher in the spring and winter than those in the summer and autumn. The PAH sources were identified by diagnostic ratio approaches and principal component analysis. E-waste dismantling was identified as the major source of PAH pollution within this area, where approximately 82.4% of the PAHs was attributed to e-waste dismantling at an industrial park (EP site). Among the sites sampled, the pollutant levels and cancer risk were highest at the EP site, and they could pose a cancer risk for humans, although only the bioaccessible PAHs in human lungs were considered. In particular, infants had a higher health risk than adults, thereby suggesting that air pollution with PAHs is a concern in this area. This study provides clear evidence of the requirement for control measurements of e-waste dismantling processes.

© 2019 Elsevier B.V. All rights reserved.

* Corresponding author.

E-mail address: antc99@gdut.edu.cn (T. An).

1. Introduction

Electronic waste or e-waste is an emerging ecological issue in all countries (Bakhiyi et al., 2018; Heacock et al., 2016). The improper disposal of e-waste leads to the potential emission of air pollutants, which are a major environmental challenge. Elevated concentrations of pollutants such as heavy metals (Huang et al., 2016), volatile organic compounds (VOCs) (An et al., 2014; Liu et al., 2017), and semi-VOCs, including polycyclic aromatic hydrocarbons (PAHs) (Zhang et al., 2011), polybrominated biphenyl ethers (Liu et al., 2019; Wang et al., 2011b); and polychlorinated biphenyls (Chen et al., 2014; Liu et al., 2019), have been reported around e-waste dismantling areas. These contaminants can adversely affect both the environment and human health (Bakhiyi et al., 2018).

PAHs are hydrocarbons that contain multiple aromatic rings. Their presence in the environment is mainly attributable to the incomplete combustion of biomass and fossil fuels (Cao et al., 2017; Huang et al., 2014b; Shen et al., 2012). PAHs are considered global pollutants due to their carcinogenic and teratogenic effects (Shrivastava et al., 2017). Moreover, PAHs can be transported via transplacental transfer from the mother to the fetus, thereby exerting adverse impacts on the fetus (Zhang et al., 2017a). During the e-waste dismantling process, the incomplete combustion of printed circuit boards at a relatively low temperature leads to the release of PAHs (Cai et al., 2018), which could be important contributors to local environmental pollution. High levels of PAHs were determined in atmospheric particulates collected from e-waste dismantling areas in China, such as Guiyu (Deng et al., 2006; Zhang et al., 2011), Taizhou (Gu et al., 2010), and Qingyuan (Chen et al., 2016b; Wang et al., 2012b; Wei et al., 2012), where the mean concentrations of total PAHs were 6–30 times and 1.5–4 times those in Hongkong (Ma et al., 2016) and Guangzhou city (Luo et al., 2015), respectively. High level exposure to PAHs among residents can cause permanent and serious health problems (Luo et al., 2015). Thus, the emission patterns of atmospheric PAHs from e-waste dismantling processes should be systematically monitored and their sources identified to facilitate subsequent health risk control.

Particulates such as PM_{2.5} (particulate matter aerodynamic diameter $\leq 2.5 \mu\text{m}$), PM₁₀, and total suspended particulates (TSP) in the air around e-waste dismantling areas are also concerns because various toxic pollutants are spread in air particulates (Ding et al., 2018). Compared with TSP and PM₁₀, PM_{2.5} has a higher deposition fraction in the human lung (Rissler et al., 2017), with a higher health risk (Luo et al., 2015). However, in most previous studies, the health risk assessments of PAHs did not consider bioaccessibility in the lung, especially with respect to e-waste dismantling areas (Kalisa et al., 2018; Zhang et al., 2011), and the air samples were collected within a short period, such as one or two seasons (Gu et al., 2010; Wei et al., 2012). Year-round PAH data were reported from e-waste dismantling areas in Qingyuan, China, from May 2010 to April 2011 (Chen et al., 2016b), but these types of studies are still rare.

Therefore, in the present study, PAH samples were collected from different PM fractions, i.e., PM_{2.5}, PM₁₀, and TSP, as well as the gaseous phase from a typical e-waste industrial park and the surrounding areas in southern China over four seasons. Samples were collected of the gaseous and particulate phases, and the corresponding PAH levels were simultaneously measured because they are beneficial for understanding the sources of PAHs. The main objectives of this study were to determine the spatiotemporal profiles of PAHs and the human health risk associated with the bioaccessibility of PAHs in the human lung. Our findings provide empirical evidence regarding the spatiotemporal profiles of PM-bound and gaseous PAHs in e-waste dismantling areas to facilitate air quality monitoring and management by local governments.

2. Materials and methods

2.1. Reagents and materials

In this study, 16 PAH isomer standards were used comprising naphthalene (Nap), acenaphthylene (Acy), acenaphthene (Ace), fluorene

(Flu), phenanthrene (Phe), anthracene (Ant), fluoranthene (FluA), pyrene (Pyr), benzo[a]anthracene (BaA), chrysene (Chr), benzo[b]fluoranthene (BbF), benzo[k]fluoranthene (BkF), benzo[a]pyrene (BaP), indeno[1,2,3-cd]pyrene (IcdP), dibenzo[a,h]anthracene (DBaA), and benzo[g,h,i]perylene (BgHiP). In addition, isotopically labeled standards were employed comprising D₈-Nap, D₁₀-Ace, D₁₀-Phe, D₁₂-Chr, and D₁₂-Perylene (D₁₂-Per). All of these standards were purchased from AccuStandard (New Haven, US). Hexamethylbenzene was purchased from Dr. Ehrenstotfer (Augsburg, Germany). All of the solvents used for extraction and instrumental analysis were gas chromatography (GC) residue grade, and they were purchased from ANPEL Laboratory Technologies (Shanghai, China).

Prior to particle and gaseous PAH sampling, quartz fiber filters (Munktell, Sweden) were baked at 450 °C for 6 h and polyurethane foam (PUF) plugs (Restek, China) were cleaned by Soxhlet extraction for 24 h.

2.2. Sample collection

The present study was conducted at a typical e-waste dismantling area in southern China. The studied site comprised an e-waste dismantling industrial park designated as the EP site and its surrounding area, which included a roadside (RS), residential area (RA), and village (VS). The Guangzhou urban area (GZ) located approximately 400 km far away from the e-waste dismantling site was selected as the control site. Particulate matter samples (PM_{2.5}, PM₁₀, and TSP) were collected simultaneously by drawing air through quartz fiber filters followed by PUF plugs using medium-volume air samplers (Guangzhou Mingye Instrument Plant, China) at 0.3 m³ min⁻¹ for approximately 8 h (from 9:00 to 17:00). Sampling occurred approximately 1.5 to 2 m above the ground. In total, 120 samples (i.e., 15 pairs of samples each for PM_{2.5}, PM₁₀, TSP, and gaseous phase) from each season were collected simultaneously on five consecutive days from April 2015 to February 2016. After collection, the samples were wrapped in pre-cleaned aluminum foil, sealed in zip-locked polyethylene bags, and then stored at -20 °C until their analysis. Additional information about the sampling sites is provided in the Supporting Information (SI), Tables S1 and S2.

2.3. Sample treatment protocols and analytical methods

The sample pretreatment and analytical methods were based on our previous studies (An et al., 2011; Sun et al., 2014). Briefly, filters and PUF plugs were Soxhlet extracted with a hexane/dichloromethane/acetone solvent mixture (2:2:1, v/v/v) for 48 h after spiking with the surrogate standards (D₈-Nap, D₁₀-Ace, D₁₀-Phe, D₁₂-Chr, and D₁₂-Per). The detailed extraction and purification procedure are provided in the SI. PAHs were analyzed using an Agilent 7890B GC coupled with a 5977C mass spectrometry by electron-impact ionization in the selected ion monitoring mode. A DB-5MS (30 m \times 0.25 mm \times 0.25 μm , J&W Scientific) capillary column was used to separate the PAHs. The detailed experimental procedures are provided in the SI.

2.4. Quality assurance and quality control

A procedural blank and one spiked sample were processed with every batch of 10 field samples. The target compounds were detected in the blank at $\leq 5\%$. The recoveries of the target compounds in the standard spiked samples and surrogate standards in field samples were 39.3%–121.1%, with a relative standard deviation $\leq 10\%$ (Table S3). A seven-point calibration curve was used to quantify individual compounds. All of the regression coefficients (R^2) exceeded 0.99 for the calibration curves. The concentrations of the target compounds in all of the field samples were corrected by subtracting the corresponding procedural blanks within the same batch, but they were not corrected for the surrogate standard recoveries.

2.5. Health risk assessment

The cancer risk due to the inhalation of PAHs as carcinogenic compounds was evaluated based on the BaP equivalent concentrations of the compounds. Due to the very high carcinogenicity of BaP, its toxic equivalency factor (TEF) was defined as 1 (Abdel-Shafy and Mansour, 2016). The PAH concentrations were converted into BaP equivalent concentrations (BaP_{eq}, carcinogenic equivalents, ng m⁻³) based on the TEF values for each PAH compound as described in a previous study (Chen et al., 2016a).

The cancer risk was assessed with Eqs. (1) and (2) by considering the bioaccessible PAHs in the human lung:

$$\text{Cancer Risk} = \sum (C_{PAHi} \times TEF_i) \times UR_{BaP} \tag{1}$$

$$\text{Cancer Risk}_{Bio} = \sum (C_{PAHi} \times Ba \times TEF_i) \times UR_{BaP} \tag{2}$$

where C_{PAHi} is the concentration of each PAH isomer, TEF_i is the TEF of the individual PAH_i based on BaP (Table 1), UR_{BaP} is the unit cancer risk factor of BaP defined as the cancer risk for a person due to inhalational exposure at a BaP equivalent concentration of 1 ng m⁻³ over a lifetime (70 years), and Ba (%) is the bioaccessibility (the maximum fraction of chemicals that can be absorbed by human organs) of PAHs in the human lung. In the present study, the value of UR_{BaP} was set as 1.1 × 10⁻⁶ ng m⁻³ (Kalisa et al., 2018), the deposition fraction of PM_{2.5} in the human lung was considered because only PAHs in PM_{2.5} deposited in the human lung are bioaccessible, and the corresponding Ba value was used as described in previous studies (Lu et al., 2018; Yu et al., 2018b).

In the noncarcinogenic risk assessment, the human daily inhalation exposure to PAHs was measured using two methods in order to obtain the estimated daily intake (EDI) (ng kg-bw⁻¹ day⁻¹) and estimated daily uptake (EDU) (ng kg-bw⁻¹ day⁻¹) by considering the bioaccessibility of PAHs in the human lung. EDI and EDU were calculated using Eqs. 3 and 4, respectively (Lu et al., 2018):

$$EDI = (C_{PAHi} \times IR) / BW \tag{3}$$

$$EDU = (C_{PAHi} \times Ba \times IR) / BW \tag{4}$$

where C_{PAHi} is the PAH concentration in PM_{2.5} or the gaseous phase, IR (m³ day⁻¹) is the inhalation rate of air, BW (kg) is the body weight,

and Ba (%) is the bioaccessibility of PAHs in the human lung. The IR, BW, and Ba parameters used in the calculations were as described in previous studies (Lu et al., 2018; Yu et al., 2018b).

2.6. Statistical analysis

Principal component analysis was used together with PAH diagnostic ratio approaches to investigate the sources of PAHs. The percentage of each pollution source in the PAH emissions was subjected to multivariate linear regression analysis. The differences between the target compound concentrations in the two groups were analyzed using the Mann-Whitney U test. For values below the limit of quantification (LOQ) but above the limit of detection, a value of LOQ/2 was assigned, as suggested previously (Lu et al., 2018).

3. Results and discussion

3.1. Seasonal mass concentration variations of TSP, PM₁₀ and PM_{2.5}

The TSP concentrations were measured as 84.8–414 μg m⁻³ within the e-waste dismantling area (Fig. 1). The highest TSP concentration was found at the EP site (190–381 μg m⁻³), followed by the RS, VS, RA, and GZ sites (131–414, 95.7–218, 84.9–158, and 78.8–153 μg m⁻³, respectively). Except for those at the EP and RS sites during the spring (381 and 414 μg m⁻³, respectively), most of the TSP levels were below the second grade threshold set by the Chinese National Ambient Air Quality Standards GB 3095-2012 (300 μg m⁻³) (CHNMEP, 2012). At the EP site, the highest TSP concentration was found in the spring, followed by the winter and autumn (290 and 269 μg m⁻³, respectively), and the lowest concentration was found in the summer (191 μg m⁻³). Similarly, the TSP concentrations at the RS, VS, RA, and GZ sites were highest in the spring (414, 218, 158, and 153 μg m⁻³, respectively) and lowest in the summer (131, 128, 84.9, and 87.7 μg m⁻³, respectively). These differences occurred because the pollutant concentrations at these sites were greatly influenced by the meteorological conditions (Chen et al., 2016b), where the particulate concentrations were greatly reduced by wet deposition due to rain in the summer.

Compared with the results obtained in previous studies, the TSP levels at the EP site were 31.8% and 105% higher than those in the e-waste dismantling areas in Qingyuan (109–314 μg m⁻³) (Chen et al., 2016b) and Guiyu (30.2–201 μg m⁻³), respectively (Deng et al., 2006). However, the TSP levels in the areas surrounding the EP site (RA and

Table 1
Carcinogenic risk calculated from BaP_{eq} based concentrations of PAHs (ng m⁻³) considering bioaccessibility in human lung.

Compound	TEF	BaP _{eq} based concentrations of PAHs (ng m ⁻³)									
		EP site		RS site		VS site		RA site		GZ site	
		Median	95th pct.	Median	95th pct.	Median	95th pct.	Median	95th pct.	Median	95th pct.
Nap	0.001	1.09 × 10 ⁻³	4.28 × 10 ⁻³	1.02 × 10 ⁻³	3.37 × 10 ⁻³	1.54 × 10 ⁻⁴	1.98 × 10 ⁻³	5.10 × 10 ⁻⁴	2.71 × 10 ⁻³	4.56 × 10 ⁻⁴	3.52 × 10 ⁻³
Acy	0.001	4.43 × 10 ⁻⁴	4.71 × 10 ⁻³	1.04 × 10 ⁻³	3.46 × 10 ⁻³	2.18 × 10 ⁻⁴	4.47 × 10 ⁻⁴	1.56 × 10 ⁻⁴	7.48 × 10 ⁻⁴	8.21 × 10 ⁻⁵	5.44 × 10 ⁻⁴
Ace	0.001	9.33 × 10 ⁻⁵	6.71 × 10 ⁻⁴	1.66 × 10 ⁻⁴	3.35 × 10 ⁻⁴	2.55 × 10 ⁻⁵	8.96 × 10 ⁻⁵	7.02 × 10 ⁻⁵	1.62 × 10 ⁻⁴	4.25 × 10 ⁻⁵	1.43 × 10 ⁻⁴
Flu	0.001	1.41 × 10 ⁻³	6.05 × 10 ⁻³	1.66 × 10 ⁻³	3.71 × 10 ⁻³	5.70 × 10 ⁻⁴	1.53 × 10 ⁻³	9.67 × 10 ⁻⁴	2.19 × 10 ⁻³	7.84 × 10 ⁻⁴	1.89 × 10 ⁻³
Phe	0.001	6.36 × 10 ⁻³	2.69 × 10 ⁻²	4.87 × 10 ⁻³	1.15 × 10 ⁻²	2.36 × 10 ⁻³	4.92 × 10 ⁻³	3.63 × 10 ⁻³	7.42 × 10 ⁻³	2.30 × 10 ⁻³	7.90 × 10 ⁻³
Ant	0.01	8.77 × 10 ⁻³	4.90 × 10 ⁻²	5.46 × 10 ⁻³	1.70 × 10 ⁻²	2.51 × 10 ⁻³	5.43 × 10 ⁻³	3.36 × 10 ⁻³	7.38 × 10 ⁻³	2.01 × 10 ⁻³	7.44 × 10 ⁻³
FluA	0.001	1.68 × 10 ⁻³	9.47 × 10 ⁻³	1.23 × 10 ⁻³	3.30 × 10 ⁻³	7.55 × 10 ⁻⁴	1.62 × 10 ⁻³	1.00 × 10 ⁻³	2.06 × 10 ⁻³	7.91 × 10 ⁻⁴	4.27 × 10 ⁻³
Pyr	0.001	1.04 × 10 ⁻³	8.02 × 10 ⁻³	7.66 × 10 ⁻⁴	1.90 × 10 ⁻³	4.41 × 10 ⁻⁴	9.12 × 10 ⁻⁴	6.63 × 10 ⁻⁴	1.34 × 10 ⁻³	5.39 × 10 ⁻⁴	3.09 × 10 ⁻³
BaA	0.1	5.26 × 10 ⁻²	1.96 × 10 ⁻¹	1.90 × 10 ⁻²	2.43 × 10 ⁻²	5.85 × 10 ⁻³	1.35 × 10 ⁻²	5.49 × 10 ⁻³	1.01 × 10 ⁻²	1.16 × 10 ⁻²	2.32 × 10 ⁻²
Chr	0.01	9.69 × 10 ⁻³	2.95 × 10 ⁻²	5.53 × 10 ⁻³	6.69 × 10 ⁻³	2.30 × 10 ⁻³	3.74 × 10 ⁻³	2.80 × 10 ⁻³	4.54 × 10 ⁻³	3.60 × 10 ⁻³	8.95 × 10 ⁻³
BbF	0.1	1.46 × 10 ⁻¹	3.73 × 10 ⁻¹	6.71 × 10 ⁻²	9.14 × 10 ⁻²	3.39 × 10 ⁻²	4.95 × 10 ⁻²	2.09 × 10 ⁻²	4.55 × 10 ⁻²	2.88 × 10 ⁻²	5.05 × 10 ⁻²
BkF	0.1	9.95 × 10 ⁻²	2.36 × 10 ⁻¹	4.72 × 10 ⁻²	7.50 × 10 ⁻²	2.23 × 10 ⁻²	3.03 × 10 ⁻²	2.12 × 10 ⁻²	3.69 × 10 ⁻²	2.83 × 10 ⁻²	4.92 × 10 ⁻²
BaP	1	6.56 × 10 ⁻¹	1.96	1.75 × 10 ⁻¹	2.36 × 10 ⁻¹	4.33 × 10 ⁻²	1.08 × 10 ⁻¹	3.03 × 10 ⁻²	7.47 × 10 ⁻²	8.60 × 10 ⁻²	1.57 × 10 ⁻¹
IcdP	0.1	2.61 × 10 ⁻¹	7.39 × 10 ⁻¹	8.39 × 10 ⁻²	1.12 × 10 ⁻¹	3.60 × 10 ⁻²	6.41 × 10 ⁻²	3.10 × 10 ⁻²	5.06 × 10 ⁻²	3.45 × 10 ⁻²	6.59 × 10 ⁻²
DBahA	5	3.95 × 10 ⁻¹	6.35 × 10 ⁻¹	5.08 × 10 ⁻¹	6.84 × 10 ⁻¹	2.03 × 10 ⁻¹	3.71 × 10 ⁻¹	1.45 × 10 ⁻¹	2.85 × 10 ⁻¹	2.15 × 10 ⁻¹	3.65 × 10 ⁻¹
BghiP	0.01	1.73 × 10 ⁻²	4.79 × 10 ⁻²	5.58 × 10 ⁻³	9.07 × 10 ⁻³	1.90 × 10 ⁻³	3.34 × 10 ⁻³	1.95 × 10 ⁻³	4.43 × 10 ⁻³	2.64 × 10 ⁻³	4.33 × 10 ⁻³
Total PAHs		1.66	4.32	9.28 × 10 ⁻¹	1.28	3.55 × 10 ⁻¹	6.60 × 10 ⁻¹	2.69 × 10 ⁻¹	5.36 × 10 ⁻¹	4.18 × 10 ⁻¹	7.52 × 10 ⁻¹
Cancer risk _{Bio} Total PAHs		1.82 × 10⁻⁶	4.75 × 10⁻⁶	1.02 × 10⁻⁶	1.41 × 10⁻⁶	0.39 × 10 ⁻⁶	0.73 × 10 ⁻⁶	0.30 × 10 ⁻⁶	0.59 × 10 ⁻⁶	0.46 × 10 ⁻⁶	0.83 × 10 ⁻⁶

The bold values indicate the carcinogenic risk are higher than USEPA value.

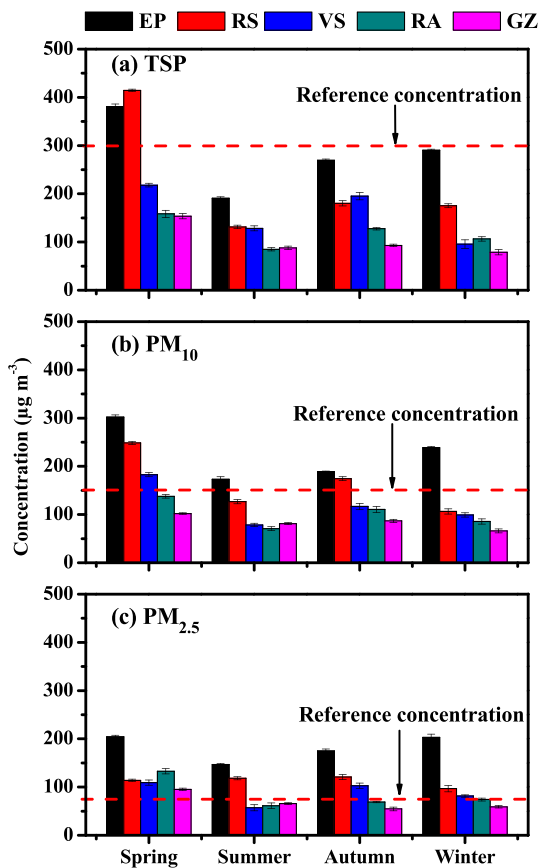


Fig. 1. Seasonal variations and spatial distribution of the concentrations of TSP (a), PM_{10} (b) and $PM_{2.5}$ (c) at different sampling sites.

VS sites) were lower than those in Qingyuan and Guiyu. These results indicated that the construction of an e-waste dismantling industrial park by the local government made a positive contribution to the reduction in TSP pollution for residents.

The concentrations of PM_{10} and $PM_{2.5}$ within the e-waste dismantling area were $70.7\text{--}302$ and $57.1\text{--}204 \mu\text{g m}^{-3}$, respectively (Fig. 1). The seasonal variations in the concentrations of PM_{10} and $PM_{2.5}$ were similar to those in TSP at the different sampling sites. For example, at the EP site, the highest $PM_{2.5}$ level was found in the spring ($204 \pm 3 \mu\text{g m}^{-3}$), followed by the winter, autumn, and summer (203 ± 7 , 174 ± 2 , and $146 \pm 2 \mu\text{g m}^{-3}$, respectively). Similar to the TSP, the seasonal variations in the concentrations of PM_{10} and $PM_{2.5}$ might have been influenced by the meteorological conditions. The spatial distributions of the PM_{10} and $PM_{2.5}$ concentrations were also similar to those of the TSP concentration, where the highest PM_{10} and $PM_{2.5}$ concentrations were found at the EP site, followed by the RS, VS, RA, and GZ sites. However, most of the $PM_{2.5}$ levels at the sampling sites were above the second grade of the Chinese National Ambient Air Quality Standards GB 3095–2012 ($75 \mu\text{g m}^{-3}$) (CHNMEP, 2012), especially at the EP and RS sites (182 ± 27 and $112 \pm 11 \mu\text{g m}^{-3}$, respectively). The high $PM_{2.5}$ levels may represent a human health risk in the e-waste dismantling area, thereby indicating that they should be considered seriously in future research.

3.2. Spatial distributions of PAHs in TSP, PM_{10} , $PM_{2.5}$, and gaseous phase

Except for Nap, the total PAH concentrations (TSP plus the gaseous phase) in the air ranged from 29.8 to 80.7 ng m^{-3} within the e-waste dismantling area (Fig. 2). The highest PAH concentration in TSP and the gaseous phase was found at the EP site (80.7 ng m^{-3}), followed by the RS, RA, VS, and GZ sites (54.9 , 35.6 , 29.8 , and 29.6 ng m^{-3} , respectively).

The PAH concentrations at the EP and RS sites were significantly higher than those at the control site (Mann-Whitney U test, $P < 0.01$), but there was no significant difference between those at the RA and control sites ($P = 0.114$). These results suggested that the e-waste dismantling process may have been an important source of PAHs at EP site, whereas other sources of PAHs such as vehicle emissions may have made important contributions at the RS site because it was located at a roadside. The PAH levels (especially in the gaseous phase) at the RA site were 19.6% higher than those at VS site, possibly because the RA site was closer to the EP site and more greatly affected by the e-waste dismantling emissions. These results suggested that the e-waste dismantling process was an important source of PAHs in the e-waste dismantling area.

The total PAH concentrations on TSP, PM_{10} , and $PM_{2.5}$ within the e-waste dismantling area were $2.9\text{--}16.1$, $2.7\text{--}15.1$, and $2.2\text{--}14.6 \mu\text{g m}^{-3}$, respectively (Fig. 2 and Table S4). There were no obvious differences in the PAH concentrations in the particulates (TSP, PM_{10} , and $PM_{2.5}$), where 72.2%–90.9% of the particulate-bound PAHs were present on $PM_{2.5}$ in this area. For instance, the PAH concentrations on TSP, PM_{10} , and $PM_{2.5}$ were 16.1 , 15.1 , and 14.6 ng m^{-3} , respectively, at the EP site. Thus, the particulate-bound PAHs within this area were dominated by fine particles and most were derived from the e-waste dismantling process. We also found that 80.1%–91.3% of the PAHs in this area were present in the gaseous phase. For example, the PAH concentrations in the gaseous phase were $64.6 \pm 9.6 \text{ ng m}^{-3}$ at the EP site. Similar results were also obtained at the control site where 82.4% of the particulate-bound PAHs were present in $PM_{2.5}$ and 88.5% in the gaseous phase. These results agree with those obtained in a previous study, which

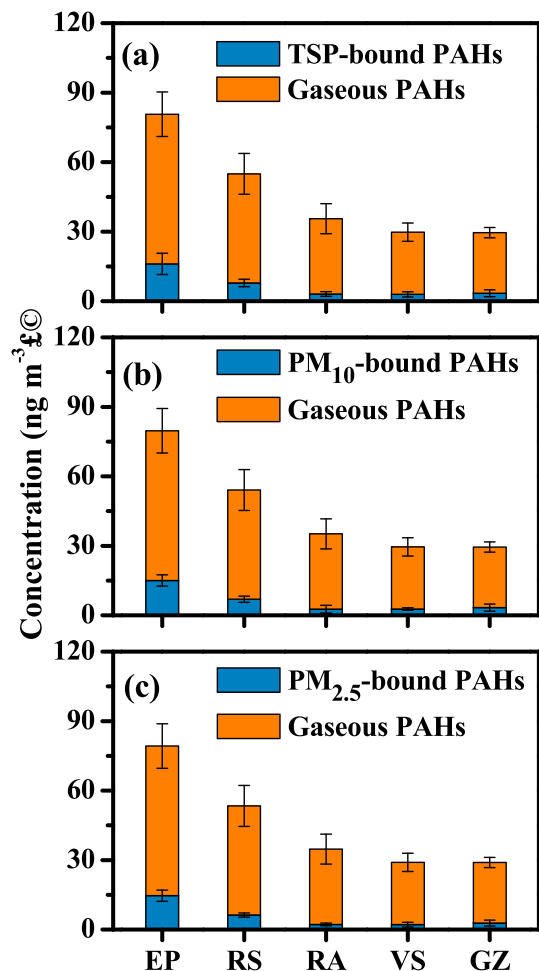


Fig. 2. Concentrations of PAHs on particulate (TSP, PM_{10} and $PM_{2.5}$) and in gaseous phase at different sampling sites.

showed that 78.9% of the PAHs were present in the gaseous phase (Huang et al., 2014a). These results demonstrated that most of the PAHs were distributed in the gaseous phase and PM_{2.5}.

The highest PAH levels on PM_{2.5} were found at the EP site, where they ranged from 2.1 to 45.0 ng m⁻³ with a median of 5.7 ng m⁻³. The PAH concentrations were lower than those determined previously in the e-waste dismantling areas at Qingyuan (27.6 ng m⁻³) (Chen et al., 2016b), Taizhou (129 ng m⁻³) (Gu et al., 2010), and Guiyu (102 ng m⁻³) (Deng et al., 2006), thereby suggesting that the construction of the e-waste dismantling industrial park had a positive effect on reducing the overall pollution with PAHs.

Among the different isomers, two- and three-ring PAHs such as Phe were mostly distributed in the gaseous phase, four ring PAHs such as FluA and Pyr were both dominant in the gaseous and particulate phases, and five and six ring PAHs were distributed mainly in the particulate phase. Phe and Pyr accounted for 70.0% ± 7.4% of the total PAHs in the gaseous phase, and BbF, BkF, IcdP, and BghiP accounted for 64.1% ± 6.5% of the total PAHs in the particulate phase (Fig. S1). These results agreed with the measurements obtained previously in a rural area of the Pearl River Delta region, China (Huang et al., 2014a), as well as in Shanghai, China and South Korea (Liu et al., 2015b; Nguyen et al., 2018). PAH isomers comprise several aromatic rings and their octanol-air partition coefficient (K_{OA}) increases with the number of rings (Zhang et al., 2011). Thus, PAH isomers with fewer rings are likely to be present in the gaseous phase, whereas those with more rings will probably be bound to particles, especially in PM_{2.5}.

3.3. Seasonal variations in PAHs in TSP, PM₁₀, PM_{2.5}, and gaseous phase

At the EP site, the highest atmospheric concentration of PAH (TSP plus the gaseous phase) was found in the spring (153 ng m⁻³), followed by the winter and autumn (52.0 and 43.1 ng m⁻³, respectively), and the lowest concentration was observed in the summer (33.2 ng m⁻³) (Fig. 3). The seasonal variations in the PAH concentrations at the RA and VS sites were similar to those at the EP site (Fig. S2), thereby suggesting that the PAHs at the RA and VS sites were influenced mainly by the EP site and that the source of the atmospheric PAHs was the e-waste dismantling process. The seasonal variations in the atmospheric PAHs at these sites might have been related to the amount of e-waste dismantling.

The seasonal variations in the PAHs at the RS site were different from those at the EP, RA, and VS sites. The concentrations of PAHs at the RS site decreased from the spring to winter, where they ranged from 39.9 to 77.9 ng m⁻³ (Fig. 3). In addition to the influence of the e-waste dismantling process, the seasonal variations in the PAHs at the RS site might have been related to the number of passing vehicles because the RS site was located at a roadside within the e-waste dismantling area, and thus this site was affected by both the e-waste dismantling process and vehicle pollution. At the GZ control site, the PAH level was highest in the spring, followed by the summer, winter, and autumn (43.1, 24.3, 22.8, and 21.7 ng m⁻³, respectively) because it was affected by different sources (Fig. S2). The variations in the concentrations of PAHs at the GZ site might also have been related to vehicle emissions because motor vehicle exhaust is the main source of PAHs in this city (Liu et al., 2015a).

The e-waste dismantling sites and control site are located in a subtropical zone, so PAH emissions due to the burning of coal for heating during the cold season could be ignored. However, the pollutant concentrations at these sites are influenced by the Asian monsoon system to some extent. In the summer and autumn, air pollutants are generally diluted and diffused because of the influence of the summer monsoon from the ocean. In the spring and winter, air pollutants from coal burning areas are transported to southern China via the influence of the winter monsoon from the mainland (Jiang et al., 2018).

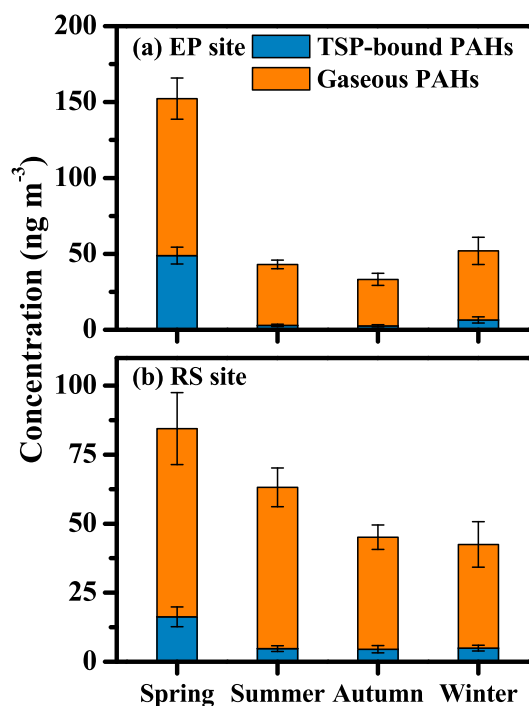


Fig. 3. Seasonal concentration variations of TSP-bound and gaseous PAHs at EP (a) and RS (b) sites.

3.4. Sources of atmospheric PAHs at different sites

The concentrations of Acy, Flu, Ant, Phe, FluA, and BghiP were significantly higher at the EP site than those at the GZ control site (Mann-Whitney U test, $P = 0-0.033$). For instance, the concentrations of Acy, Ant, and Phe at the EP site were 7.5, 4.8, and 2.7 times those at the control site, respectively (Fig. S3). These results suggested that the characteristic isomers emitted by the e-waste dismantling process comprised low-ring PAHs, which was consistent with the fact that low molecular weight PAH isomers dominate during the pyrolytic processing of e-waste at 320 °C (Cai et al., 2018). Therefore, the low molecular weight PAH isomers such as three to four ring PAHs may have originated from the e-waste dismantling process within this area.

In addition to the EP site, the concentrations of BbF, DBaH, and IcdP at the RS site were significantly higher than those at the control site ($P = 0-0.007$). For example, the concentration of IcdP at RS was 2.3 times that at the control site (Fig. S3). The RS site was located close to a road and BbF, DBaH, and IcdP are the dominant isomers from vehicle emissions (Keyte et al., 2016). These results indicated that vehicle emissions must have been an important source of PAHs at the RS site together with the main contribution from the e-waste dismantling process.

The ratios of Ant/(Ant + Phe), FluA/(FluA + Pyr), BaA/(BaA + Chr), IcdP/(IcdP + BghiP), BbF/(BbF + BkF), and BaP/(BaP + BghiP) are usually analyzed to investigate the sources of atmospheric PAHs (Cai et al., 2018). Among these six isomer pairs, FluA/(FluA + Pyr) and IcdP/(IcdP + BghiP) are the most conservative diagnostic ratios used to identify the sources of atmospheric PAHs (Tobiszewski and Namiesnik, 2012). According to previous studies (Lin et al., 2015; Wang et al., 2011a), FluA/(FluA + Pyr) > 0.5 or IcdP/(IcdP + BghiP) > 0.5 indicated that PAHs were derived mainly from biomass and coal combustion, whereas $0.4 \leq \text{FluA}/(\text{FluA} + \text{Pyr}) \leq 0.5$ or $0.2 \leq \text{IcdP}/(\text{IcdP} + \text{BghiP}) \leq 0.5$ indicated that the PAHs came mainly from petroleum combustion. In the present study, the FluA/(FluA + Pyr) and IcdP/(IcdP + BghiP) ratios at the EP site were both above 0.5 (Fig. 4), thereby indicating that the PAHs at the EP site were derived mainly from coal and biomass combustion. Similar results were obtained at the RS, VS, RA, and GZ sites.

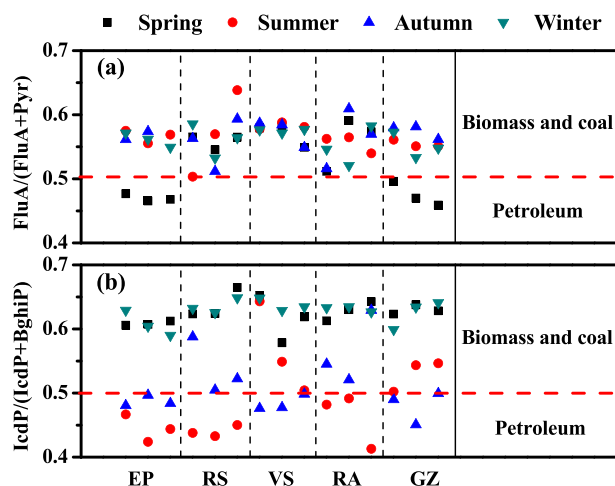


Fig. 4. Seasonal variation of FluA/(FluA+Pyr) (a) and IcdP/(IcdP+BghiP) (b) at different sampling sites.

These results agreed with the previously reported mechanisms for the formation of PAHs from the combustion of coal, biomass, and plastics (Ross et al., 2011; Vejerano et al., 2013; Williams et al., 2012). In particular, the volatiles released from the combustion and pyrolysis of coal, biomass, and plastics typically comprise CO, H₂, CO₂, and hydrocarbons, such as ethylene and isobutene (Iniguez et al., 2018; Wijayanta et al., 2012). PAHs are generated from these compounds via cyclopentadienyl radical recombination and other formation mechanisms (Vejerano et al., 2013). However, the determinations of the sources of PAHs in previous studies did not consider the e-waste dismantling process (Cai et al., 2018). In the present study, the PAHs were derived from coal and biomass combustion within the e-waste dismantling area, although the e-waste dismantling process was performed most extensively with no other activities within this area. At the EP site, the burning of coal could be ignored and the dismantling of devices such as printed circuit boards containing organic plastics with a similar biomass composition occurred during the dismantling process. Therefore, the PAHs at the RS, VS, and RA sites appeared to have originated from the same sources as those at the EP site, with typical characteristic contributions from coal and biomass combustion in the e-waste dismantling process, and the PAHs spread to the other three sites from within the e-waste dismantling area.

Principal component analysis was conducted to further analyze the PAH sources in the study areas and two principal components (PCs) were identified at the EP site (Table S5). PC1 explained 71.2% of the variance and it was due to three to four ring PAHs, including Phe, FluA, and Pyr, which are mainly derived from coal and biomass combustion (Shen et al., 2013; Yang et al., 2010). However, the PAHs derived from coal and biomass combustion came mainly from the e-waste dismantling process within the e-waste dismantling sites. Therefore, PC1 was mainly related to the e-waste dismantling process in the study area. PC2 accounted for 24.6% of the total variance. PC2 had high positive loadings for high-ring PAHs, including BkF, IcdP, and BghiP, which are characteristic compounds in vehicle emissions (Li et al., 2018; Zhou et al., 2019). Three PCs were obtained for the RS, VS, RA, and GZ sites (Table S5). Similar to the EP site, PC1 was related to the e-waste dismantling process for the RS, VS, and RA sites, and coal and biomass combustion for the GZ site. PC2 was attributable to vehicle emissions at all of the sites. PC3 was due to coal coking and highly loaded for Acy and Flu, which were consistent with the characteristics of coal coking being dominated by two to three ring PAHs (Mu et al., 2014).

Furthermore, multivariate linear regression was conducted to determine the contributions of PC1, PC2, and PC3 to the total PAHs at different sites. At the EP site, PC1 (e-waste dismantling processes) accounted for 82.7% of the total PAHs and PC2 (vehicle emission) accounted for

17.3% (Fig. 5). Similarly, PC1, PC2, and PC3 (coking) accounted for 69.7%, 19.4%, and 10.9% at the RA site, respectively, and 69.3%, 14.8%, and 15.9% at the VS site, where they mainly originated from the EP site together with local contributions. The PAHs at the RA and VS sites were mainly determined by the e-waste dismantling process because they were close to the EP site and within the same e-waste dismantling area with similar patterns in terms of the contributions of different PAHs. The results obtained from the RS site were similar to those at the GZ site, where PC1, PC2, and PC3 explained 55.2%, 28.8%, and 16.0% of the variation for the former, respectively, and 52.1%, 34.3%, and 13.6% for the latter. The PAHs at the RS site were mainly determined by the e-waste dismantling process, but vehicle emissions were still important. However, the GZ site was mainly affected by coal and biomass combustion, and vehicle emissions. These results were consistent with those calculated using the diagnostic ratio source analysis method. Both methods demonstrated that the main source of atmospheric PAHs was the e-waste dismantling process within this area.

3.5. Health risk assessment and human daily exposure to PAHs

The median and 95th percentile of the BaP_{eq} concentrations for the total PAHs in PM_{2.5} and the gaseous phase were used to calculate the “median” and “high” cancer risks. The “median” and “high” cancer risks at the sampling sites were 0.54×10^{-6} to 3.03×10^{-6} and 1.16×10^{-6} to 7.82×10^{-6} , respectively (Table S6). When the bioaccessibilities of PAHs were included in the calculations, the corresponding “median” and “high” cancer risks decreased to 0.30×10^{-6} to 1.82×10^{-6} and 0.59×10^{-6} to 4.75×10^{-6} , respectively (Table 1). The EP site had the highest “median” cancer risk (1.82×10^{-6}) and it was slightly higher than the USEPA limit (1.0×10^{-6}) (Kalisa et al., 2018), although the bioaccessibilities of the PAHs were considered. The “high” cancer risks at the VS, RA, and GZ (control) sites (0.73×10^{-6} , 0.59×10^{-6} , and 0.83×10^{-6} , respectively) were all lower than 1.0×10^{-6} , and the “median” cancer risk at the RS site (1.02×10^{-6}) was slightly higher than 1.0×10^{-6} . These results suggested that the PAH pollution at the EP and RS sites could pose a cancer risk to humans via inhalation, whereas only small cancer risks were found at the VS, RA, and GZ (control) sites. The e-waste dismantling process was the main source of the risk at the EP site, and the VS, RA, and RS sites were still within the same area and they were greatly influenced by the EP site. Furthermore, the cancer risk at the EP site was 4.0–5.7 times that at the control site. However, the cancer risk at the EP site (1.78×10^{-6} in the winter) was much lower than those reported in villages (53.5×10^{-6}) and towns (45.5×10^{-6}) in Taiyuan (Duan et al., 2014) as well as in Beijing during the winter (8.4×10^{-6}) (Yu et al., 2018a). The burning of coal for heating in northern China during the winter usually increases the PAH emissions (Yu et al., 2018a). These results indicated that the risk of cancer when exposed to PAHs predominantly derived from the e-waste dismantling process in southern China was much lower than that from the burning of coal for heating in northern China, although e-waste dismantling was considered a major concern in many previous studies.

Considering the potential health risks at these sites, especially the EP site, the “median” and “high” EDI and EDU for humans via inhalation at various ages were calculated based on the median and 95th percentile for the total BaP_{eq} concentrations of PAHs in PM_{2.5} and the gaseous phase. As shown in Tables 2, S7, S8, and S9, the “median” and “high” EDI levels at the sampling sites were 0.10–1.64 and 0.22–4.22 ng kg-bw⁻¹ day⁻¹, respectively. When the bioaccessibilities of PAHs were included in the calculations, the corresponding “median” and “high” EDU values decreased to 0.05–1.03 and 0.10–2.69 ng kg-bw⁻¹ day⁻¹, respectively. People living at the EP site had the highest EDI and EDU values, followed by those at the RS, GZ, VS, and RA sites. For example, the “high” EDU levels at the EP and RS sites for PM_{2.5} were 0.69–2.45 and 0.15–0.53 ng kg-bw⁻¹ day⁻¹, respectively (Table 2). We also found that although over 70% of the PAHs were present in the gaseous phase in these areas, the EDI and EDU values for BaP_{eq} PAHs in the gaseous

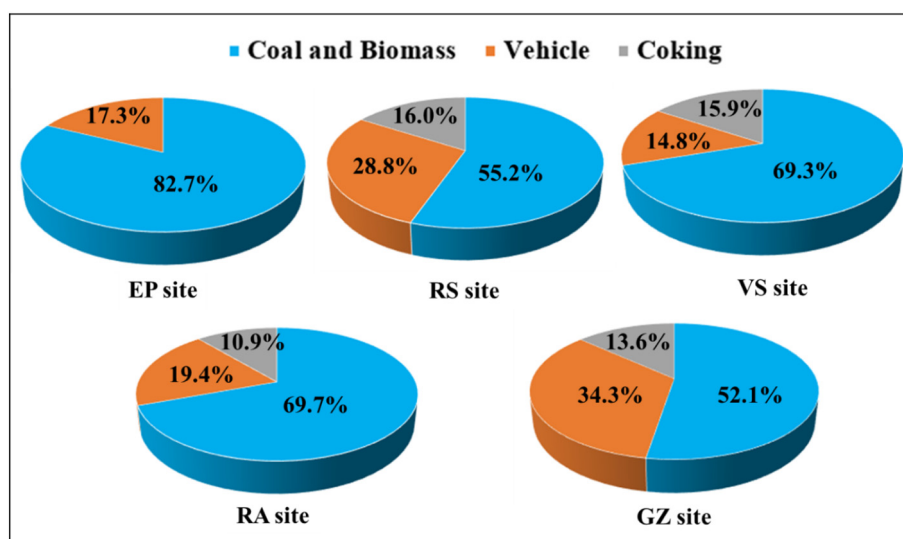


Fig. 5. Source contributions (%) of PAHs at different sampling sites.

phase ($0.01\text{--}0.61\text{ ng kg-bw}^{-1}\text{ day}^{-1}$) were lower than those for $\text{PM}_{2.5}$ ($0.05\text{--}3.67\text{ ng kg-bw}^{-1}\text{ day}^{-1}$). These results were attributed to the high toxicity of high-ring PAHs bound to $\text{PM}_{2.5}$, but the levels of the high-ring numbered bioaccessible PAHs in $\text{PM}_{2.5}$ (54%–69%) (Lu et al., 2018; Rissler et al., 2017) were higher than those in the gaseous phase (21%–46%) in the human lung (Yu et al., 2018b). Infants (<1-year old) had the highest EDI and EDU values in the e-waste dismantling area with 2–3 times those found in adults (>18 years old) at the control site, mainly because infants have a larger air inhalation rate to body weight ratio due to their higher oxygen demand (Lu et al., 2018). Thus, the present study indicated that infants had much higher potential health risks due to PAHs than adults.

It should be noted that our assessment had some limitations. First, the indoor PAH concentrations are generally higher than those determined outdoors (Li et al., 2019; Oliveira et al., 2016). However, our assessment only considered exposure due to the inhalation of outdoor PAH pollution, and thus we underestimated the exposure to PAHs. Second, other intake pathways were not considered, such as oral ingestion (dietary) (Wang et al., 2012a; Yu et al., 2012), dermal contact (dust) (Zhang et al., 2017b), and dermal absorption (air) (Lao et al., 2018; Weschler et al., 2015), which also led to underestimates of the human exposure to PAHs in the present study. Third, people were only present in the e-waste dismantling industrial park for 10 h (working hours) each day and they lived in the residential

area (RA site) for the remainder of the time. Thus, considering the duration of exposure during the working day, the “median” and “high” cancer risks for the EP site decreased from 1.82×10^{-6} and 4.75×10^{-6} to 1.03×10^{-6} and 2.46×10^{-6} , respectively. Similarly, the “median” and “high” EUI levels decreased from 0.30 to 1.03 and 0.78–2.69 $\text{ng kg-bw}^{-1}\text{ day}^{-1}$ to 0.15–0.52 and 0.38–1.31 $\text{ng kg-bw}^{-1}\text{ day}^{-1}$, respectively. The bioaccessibilities of PAHs in the gaseous phase were considered based on our previous study of cigarette smoke (Yu et al., 2018b), whereas those for $\text{PM}_{2.5}$ were based on the fraction deposited in the lung (Rissler et al., 2017) and without considering the PAH species. All of the factors mentioned above influenced our assessment. Thus, more studies are required in the e-waste dismantling area in order to accurately estimate the human health risk due to PAHs.

4. Conclusion

This study investigated the levels of pollution with TSP, PM_{10} , $\text{PM}_{2.5}$, and the corresponding PAHs, as well as gaseous PAHs, in an e-waste dismantling area in southern China. The concentrations of these pollutants were significantly higher at the e-waste dismantling park (EP site) than those at the control site. Most of the atmospheric PAHs were present in the gaseous phase and most of the particulate-bound PAHs were present in $\text{PM}_{2.5}$. The pollutant levels were lower in the summer and autumn than those in the spring and winter. Due to the similar compositions of the organic plastics in e-waste (printed circuit boards) and biomass, the e-waste dismantling process was identified as the main source of PAHs in this area. Human inhalation analysis showed that although bioaccessible PAHs in the human lung were considered, PAHs could pose a cancer risk to humans at the EP site. Thus, the e-waste dismantling process is an important source of PAHs and greater efforts should be made to decrease pollution with PAHs during e-waste dismantling.

Acknowledgements

This work was supported by the National Natural Science Foundation of China (41731279, 41703092 and 41425015), Local Innovative and Research Teams Project of Guangdong Pearl River Talents Program (2017BT01Z032), the Innovation Team Project of Guangdong Provincial Department of Education (2017KCXTD012) and Leading Scientific, Technical and Innovation Talents of Guangdong special support program (2016TX03Z094).

Table 2

The estimated inhalation exposure and estimated deposition dose of total PAHs on $\text{PM}_{2.5}$ in EP and RS site

Groups (years)	95th percentile BaP_{eq} concentrations of PAHs ($\text{ng kg-bw}^{-1}\text{ day}^{-1}$)							
	EP site				RS site			
	EDI		EDU		EDI		EDU	
	Male	Female	Male	Female	Male	Female	Male	Female
<1	3.668	3.555	2.311	2.453	0.796	0.772	0.502	0.532
1–3	3.062	2.975	1.929	2.053	0.665	0.646	0.419	0.446
3–6	3.205	3.513	2.019	2.424	0.696	0.763	0.438	0.526
6–9	2.471	2.401	1.557	1.657	0.537	0.521	0.338	0.360
9–12	2.345	2.275	1.478	1.570	0.509	0.494	0.321	0.341
12–15	1.968	1.635	1.240	1.128	0.427	0.355	0.269	0.245
15–18	1.756	1.535	1.106	1.059	0.381	0.333	0.240	0.230
18–44	1.734	1.632	1.041	1.077	0.377	0.354	0.226	0.234
45–59	1.716	1.577	0.926	0.946	0.372	0.342	0.201	0.205
60–79	1.426	1.443	0.770	0.866	0.310	0.313	0.167	0.188
>80	1.283	1.387	0.693	0.832	0.279	0.301	0.150	0.181

EDI: estimated daily intake; EDU: estimated daily uptake.

Appendix A. Supplementary data

Supplementary data to this article can be found online at <https://doi.org/10.1016/j.scitotenv.2019.04.385>.

References

- Abdel-Shafy, H.I., Mansour, M.S.M., 2016. A review on polycyclic aromatic hydrocarbons: source, environmental impact, effect on human health and remediation. *Egypt. J. Petrol.* 25, 107–123.
- An, T., Qiao, M., Li, G., Sun, H., Zeng, X., Fu, J., 2011. Distribution, sources, and potential toxicological significance of PAHs in drinking water sources within the Pearl River Delta. *J. Environ. Monitor.* 13, 1457–1463.
- An, T., Huang, Y., Li, G., He, Z., Chen, J., Zhang, C., 2014. Pollution profiles and health risk assessment of VOCs emitted during e-waste dismantling processes associated with different dismantling methods. *Environ. Int.* 73, 186–194.
- Bakhiyi, B., Gravel, S., Ceballos, D., Flynn, M.A., Zayed, J., 2018. Has the question of e-waste opened a Pandora's box? An overview of unpredictable issues and challenges. *Environ. Int.* 110, 173–192.
- Cai, C., Yu, S., Li, X., Liu, Y., Tao, S., Liu, W., 2018. Emission characteristics of polycyclic aromatic hydrocarbons from pyrolytic processing during dismantling of electronic wastes. *J. Hazard. Mater.* 351, 270–276.
- Cao, X.Y., Hao, X.W., Shen, X.B., Jiang, X., Wu, B.B., Yao, Z.L., 2017. Emission characteristics of polycyclic aromatic hydrocarbons and nitro-polycyclic aromatic hydrocarbons from diesel trucks based on on-road measurements. *Atmos. Environ.* 148, 190–196.
- Chen, S., Tian, M., Zheng, J., Zhu, Z., Luo, Y., Luo, X., Mai, B., 2014. Elevated levels of polychlorinated biphenyls in plants, air, and soils at an e-waste site in Southern China and enantioselective biotransformation of chiral PCBs in plants. *Environ. Sci. Technol.* 48, 3847–3855.
- Chen, J., Zhang, D., Li, G., An, T., Fu, J., 2016a. The health risk attenuation by simultaneous elimination of atmospheric VOCs and POPs from an e-waste dismantling workshop by an integrated de-dusting with decontamination technique. *Chem. Eng. J.* 301, 299–305.
- Chen, S., Wang, J., Wang, T., Wang, T., Mai, B., Simonich, S.L.M., 2016b. Seasonal variations and source apportionment of complex polycyclic aromatic hydrocarbon mixtures in particulate matter in an electronic waste and urban area in South China. *Sci. Total Environ.* 573, 115–122.
- CHNMEP, 2012. Ambient Air Quality Standards of China.
- Deng, W., Louie, P.K.K., Liu, W., Bi, X., Fu, J., Wong, M., 2006. Atmospheric levels and cytotoxicity of PAHs and heavy metals in TSP and PM_{2.5} at an electronic waste recycling site in southeast China. *Atmos. Environ.* 40, 6945–6955.
- Ding, N., Chen, S., Wang, T., Wang, T., Mai, B., 2018. Halogenated flame retardants (HFRs) and water-soluble ions (WSIs) in fine particulate matter (PM_{2.5}) in three regions of South China. *Environ. Pollut.* 238, 823–832.
- Duan, X., Wang, B., Zhao, X., Shen, G., Xia, Z., Huang, N., Jiang, Q., Lu, B., Xu, D., Fang, J., Tao, S., 2014. Personal inhalation exposure to polycyclic aromatic hydrocarbons in urban and rural residents in a typical northern city in China. *Indoor Air* 24, 464–473.
- Gu, Z., Feng, J., Han, W., Wu, M., Fu, J., Sheng, G., 2010. Characteristics of organic matter in PM_{2.5} from an e-waste dismantling area in Taizhou, China. *Chemosphere* 80, 800–806.
- Heacock, M., Kelly, C.B., Asante, K.A., Birnbaum, L.S., Bergman, A.L., Brune, M.N., Buka, I., Carpenter, D.O., Chen, A.M., Huo, X., Kamel, M., Landrigan, P.J., Magalini, F., Diaz-Barriga, F., Neira, M., Omar, M., Pascale, A., Ruchirawat, M., Sly, L., Sly, P.D., Van den Berg, M., Suk, W.A., 2016. E-waste and harm to vulnerable populations: a growing global problem. *Environ. Health Perspect.* 124, 550–555.
- Huang, B., Liu, M., Bi, X., Chaemfa, C., Ren, Z., Wang, X., Sheng, G., Fu, J., 2014a. Phase distribution, sources and risk assessment of PAHs, NPAHs and OPAHs in a rural site of Pearl River Delta region, China. *Atmos. Pollut. Res.* 5, 210–218.
- Huang, W., Huang, B., Bi, X., Lin, Q., Liu, M., Ren, Z., Zhang, G., Wang, X., Sheng, G., Fu, J., 2014b. Emission of PAHs, NPAHs and OPAHs from residential honeycomb coal briquette combustion. *Energy Fuel* 28, 636–642.
- Huang, C.L., Bao, L.J., Luo, P., Wang, Z.Y., Li, S.M., Zeng, E.Y., 2016. Potential health risk for residents around a typical e-waste recycling zone via inhalation of size-fractionated particle-bound heavy metals. *J. Hazard. Mater.* 317, 449–456.
- Iniguez, M.E., Conesa, J.A., Fullana, A., 2018. Effect of sodium chloride and thiourea on pollutant formation during combustion of plastics. *Energies* 11, 2014.
- Jiang, Y., Lin, T., Wu, Z., Li, Y., Li, Z., Guo, Z., Yao, X., 2018. Seasonal atmospheric deposition and air-sea gas exchange of polycyclic aromatic hydrocarbons over the Yangtze River Estuary, East China Sea: implications for source-sink processes. *Atmos. Environ.* 178, 31–40.
- Kalisa, E., Nagato, E.G., Bizuru, E., Lee, K.C., Tang, N., Pointing, S.B., Hayakawa, K., Archer, S.D.J., Lacap-Bugler, D.C., 2018. Characterization and risk assessment of atmospheric PM_{2.5} and PM₁₀ particulate-bound PAHs and NPAHs in Rwanda, Central-East Africa. *Environ. Sci. Technol.* 52, 12179–12187.
- Keyte, I.J., Albinet, A., Harrison, R.M., 2016. On-road traffic emissions of polycyclic aromatic hydrocarbons and their oxy- and nitro-derivative compounds measured in road tunnel environments. *Sci. Total Environ.* 566, 1131–1142.
- Lao, J.Y., Bao, L.J., Zeng, E.Y., 2018. Importance of dermal absorption of polycyclic aromatic hydrocarbons derived from barbecue fumes (vol 52, pg 8330, 2018). *Environ. Sci. Technol.* 52, 11439–11440.
- Li, X., Zheng, Y., Guan, C., Cheung, C.S., Huang, Z., 2018. Effect of biodiesel on PAH, OPAH, and NPAH emissions from a direct injection diesel engine. *Environ. Sci. Pollut. Res.* 25, 34131–34138.
- Li, T., Wang, Y., Hou, J., Zheng, D., Wang, G., Hu, C., Xu, T., Cheng, J., Yin, W., Mao, X., Wang, L., He, Z., Yuan, J., 2019. Associations between inhaled doses of PM_{2.5}-bound polycyclic aromatic hydrocarbons and fractional exhaled nitric oxide. *Chemosphere* 218, 992–1001.
- Lin, Y., Ma, Y.Q., Qiu, X.H., Li, R., Fang, Y.H., Wang, J.X., Zhu, Y.F., Hu, D., 2015. Sources, transformation, and health implications of PAHs and their nitrated, hydroxylated, and oxygenated derivatives in PM_{2.5} in Beijing. *J. Geophys. Res.* 120, 7219–7228.
- Liu, J., Man, R., Ma, S., Li, J., Wu, Q., Peng, J., 2015a. Atmospheric levels and health risk of polycyclic aromatic hydrocarbons (PAHs) bound to PM_{2.5} in Guangzhou, China. *Mar. Pollut. Bull.* 100, 134–143.
- Liu, Y., Wang, S., Lohmann, R., Yu, N., Zhang, C., Gao, Y., Zhao, J., Ma, L., 2015b. Source apportionment of gaseous and particulate PAHs from traffic emission using tunnel measurements in Shanghai, China. *Atmos. Environ.* 107, 129–136.
- Liu, R., Chen, J., Li, G., An, T., 2017. Using an integrated decontamination technique to remove VOCs and attenuate health risks from an e-waste dismantling workshop. *Chem. Eng. J.* 318, 57–63.
- Liu, R., Ma, S., Li, G., Yu, Y., An, T., 2019. Comparing pollution patterns and human exposure to atmospheric PBDEs and PCBs emitted from different e-waste dismantling processes. *J. Hazard. Mater.* 369, 142–149.
- Lu, S., Kang, L., Liao, S., Ma, S., Zhou, L., Chen, D., Yu, Y., 2018. Phthalates in PM_{2.5} from Shenzhen, China and human exposure assessment factored their bioaccessibility in lung. *Chemosphere* 202, 726–732.
- Luo, P., Bao, L.J., Li, S.M., Zeng, E.Y., 2015. Size-dependent distribution and inhalation cancer risk of particle-bound polycyclic aromatic hydrocarbons at a typical e-waste recycling and an urban site. *Environ. Pollut.* 200, 10–15.
- Ma, Y., Cheng, Y., Qiu, X., Lin, Y., Cao, J., Hu, D., 2016. A quantitative assessment of source contributions to fine particulate matter (PM_{2.5})-bound polycyclic aromatic hydrocarbons (PAHs) and their nitrated and hydroxylated derivatives in Hong Kong. *Environ. Pollut.* 219, 742–749.
- Mu, L., Peng, L., Liu, X., Song, C., Bai, H., Zhang, J., Hu, D., He, Q., Li, F., 2014. Characteristics of polycyclic aromatic hydrocarbons and their gas/particle partitioning from fugitive emissions in coke plants. *Atmos. Environ.* 83, 202–210.
- Nguyen, T.N.T., Jung, K.-S., Son, J.M., Kwon, H.O., Choi, S.D., 2018. Seasonal variation, phase distribution, and source identification of atmospheric polycyclic aromatic hydrocarbons at a semi-rural site in Ulsan, South Korea. *Environ. Pollut.* 236, 529–539.
- Oliveira, M., Slezakova, K., Delerue-Matos, C., Pereira, M.d.C., Morais, S., 2016. Assessment of polycyclic aromatic hydrocarbons in indoor and outdoor air of preschool environments (3–5 years old children). *Environ. Pollut.* 208, 382–394.
- Rissler, J., Gudmundsson, A., Nicklasson, H., Swietlicki, E., Wollmer, P., Londahl, J., 2017. Deposition efficiency of inhaled particles (15–5000 nm) related to breathing pattern and lung function: an experimental study in healthy children and adults. *Part. Fibre Toxicol.* 14. <https://doi.org/10.1186/s12989-017-0190-8>.
- Ross, A.B., Bartle, K.D., Hall, S., Jones, J.M., Williams, A., Kubica, K., Fynes, G., Owen, A., 2011. Formation and emission of polycyclic aromatic hydrocarbon soot precursors during coal combustion. *J. Energy Inst.* 84, 220–226.
- Shen, G., Tao, S., Wei, S., Zhang, Y., Wang, R., Wang, B., Li, W., Shen, H., Huang, Y., Chen, Y., Chen, H., Yang, Y., Wang, W., Wang, X., Liu, W., Simonich, S.L., 2012. Emissions of parent, nitro, and oxygenated polycyclic aromatic hydrocarbons from residential wood combustion in rural China. *Environ. Sci. Technol.* 46, 8123–8130.
- Shen, G., Tao, S., Wei, S., Chen, Y., Zhang, Y., Shen, H., Huang, Y., Zhu, D., Yuan, C., Wang, H., Wang, Y., Pei, L., Liao, Y., Duan, Y., Wang, B., Wang, R., Lv, Y., Li, W., Wang, X., Zheng, X., 2013. Field measurement of emission factors of PM, EC, OC, parent, nitro-, and oxy-polycyclic aromatic hydrocarbons for residential briquette, coal cake, and wood in rural Shanxi, China. *Environ. Sci. Technol.* 47, 2998–3005.
- Shrivastava, M., Lou, S., Zelenyuk, A., Easter, R.C., Corley, R.A., Thrall, B.D., Rasch, P.J., Fast, J.D., Massey Simonich, S.L., Shen, H., Tao, S., 2017. Global long-range transport and lung cancer risk from polycyclic aromatic hydrocarbons shielded by coatings of organic aerosol. *Proc. Natl. Acad. Sci. U. S. A.* 114, 1246–1251.
- Sun, H., An, T., Li, G., Qiao, M., Wei, D., 2014. Distribution, possible sources, and health risk assessment of SVOC pollution in small streams in Pearl River Delta, China. *Environ. Sci. Pollut. Res.* 21, 10083–10095.
- Tobiszewski, M., Namiesnik, J., 2012. PAH diagnostic ratios for the identification of pollution emission sources. *Environ. Pollut.* 162, 110–119.
- Vejerano, E.P., Holder, A.L., Marr, L.C., 2013. Emissions of polycyclic aromatic hydrocarbons, polychlorinated dibenzo-p-dioxins, and dibenzofurans from incineration of nanomaterials. *Environ. Sci. Technol.* 47, 4866–4874.
- Wang, W., Jariyasopit, N., Schrlau, J., Jia, Y., Tao, S., Yu, T.W., Dashwood, R.H., Zhang, W., Wang, X., Simonich, S.L., 2011a. Concentration and photochemistry of PAHs, NPAHs, and OPAHs and toxicity of PM_{2.5} during the Beijing Olympic Games. *Environ. Sci. Technol.* 45, 6887–6895.
- Wang, Z.J., Xu, Y., Shao, J.H., Wang, J., Li, R.H., 2011b. Genes associated with 2-methylisoborneol biosynthesis in cyanobacteria: isolation, characterization, and expression in response to light. *PLoS One* 6. <https://doi.org/10.1371/journal.pone.0018665>.
- Wang, D., Yu, Y., Zhang, X., Zhang, S., Pang, Y., Zhang, X., Yu, Z., Wu, M., Fu, J., 2012a. Polycyclic aromatic hydrocarbons and organochlorine pesticides in fish from Taihu Lake: their levels, sources, and biomagnification. *Ecotoxicol. Environ. Saf.* 82, 63–70.
- Wang, J., Chen, S., Tian, M., Zheng, X., Gonzales, L., Ohura, T., Mai, B., Simonich, S.L.M., 2012b. Inhalation cancer risk associated with exposure to complex polycyclic aromatic hydrocarbon mixtures in an electronic waste and urban area in South China. *Environ. Sci. Technol.* 46, 9745–9752.
- Wei, S., Huang, B., Liu, M., Bi, X., Ren, Z., Sheng, G., Fu, J., 2012. Characterization of PM_{2.5}-bound nitrated and oxygenated PAHs in two industrial sites of South China. *Atmos. Res.* 109–110, 76–83.
- Weschler, C.J., Beko, G., Koch, H.M., Salthammer, T., Schripp, T., Toftum, J., Clausen, G., 2015. Transdermal uptake of diethyl phthalate and Di(n-butyl) phthalate directly from air: experimental verification. *Environ. Health Perspect.* 123, 928–934.

- Wijayanta, A.T., Saiful Alam, M., Nakaso, K., Fukai, J., Shimizu, M., 2012. Optimized combustion of biomass volatiles by varying O₂ and CO₂ levels: a numerical simulation using a highly detailed soot formation reaction mechanism. *Bioresour. Technol.* 110, 645–651.
- Williams, A., Jones, J.M., Ma, L., Pourkashanian, M., 2012. Pollutants from the combustion of solid biomass fuels. *Prog. Energy Combust. Sci.* 38, 113–137.
- Yang, X.Y., Igarashi, K., Tang, N., Lin, J.M., Wang, W., Kameda, T., Toriba, A., Hayakawa, K., 2010. Indirect- and direct-acting mutagenicity of diesel, coal and wood burning-derived particulates and contribution of polycyclic aromatic hydrocarbons and nitropolycyclic aromatic hydrocarbons. *Mutat. Res. Genet. Toxicol. Environ. Mutagen.* 695, 29–34.
- Yu, Y., Chen, L., Yang, D., Pang, Y., Zhang, S., Zhang, X., Yu, Z., Wu, M., Fu, J., 2012. Polycyclic aromatic hydrocarbons in animal-based foods from Shanghai: bioaccessibility and dietary exposure. *Food Addit. Contam., Part A* 29, 1465–1474.
- Yu, Q., Yang, W., Zhu, M., Gao, B., Li, S., Li, G., Fang, H., Zhou, H., Zhang, H., Wu, Z., Song, W., Tan, J., Zhang, Y., Bi, X., Chen, L., Wang, X., 2018a. Ambient PM_{2.5}-bound polycyclic aromatic hydrocarbons (PAHs) in rural Beijing: unabated with enhanced temporary emission control during the 2014 APEC summit and largely aggravated after the start of wintertime heating. *Environ. Pollut.* 238, 532–542.
- Yu, Y., Jiang, Z., Zhao, Z., Chong, D., Li, G., Ma, S., Zhang, Y., An, T., 2018b. Novel in vitro method for measuring the mass fraction of bioaccessible atmospheric polycyclic aromatic hydrocarbons using simulated human lung fluids. *Environ. Pollut.* 242, 1633–1641.
- Zhang, D., An, T., Qiao, M., Loganathan, B.G., Zeng, X., Sheng, G., Fu, J., 2011. Source identification and health risk of polycyclic aromatic hydrocarbons associated with electronic dismantling in Guiyu town, South China. *J. Hazard. Mater.* 192, 1–7.
- Zhang, X., Li, X., Jing, Y., Fang, X., Zhang, X., Lei, B., Yu, Y., 2017a. Transplacental transfer of polycyclic aromatic hydrocarbons in paired samples of maternal serum, umbilical cord serum, and placenta in Shanghai, China. *Environ. Pollut.* 222, 267–275.
- Zhang, X., Yu, Y., Gu, Y., Li, X., Zhang, X., Yu, Y., 2017b. In vitro determination of transdermal permeation of synthetic musks and estimated dermal uptake through usage of personal care products. *Chemosphere* 173, 417–424.
- Zhou, S., Zhou, J., Zhu, Y., 2019. Chemical composition and size distribution of particulate matters from marine diesel engines with different fuel oils. *Fuel* 235, 972–983.